PHYSICAL REVIEW B VOLUME 29, NUMBER 12 15 JUNE 1984

Highly conducting polyparaphenylene, polypyrrole, and polythiophene chains: An *ab initio* study of the geometry and electronic-structure modifications upon doping

J. L. Brédas, B. Thémans, J. G. Fripiat, and J. M. André
Laboratoire de Chimie Théorique Appliquée, Facultés Universitaires Notre-Dame de la Paix, rue de Bruxelles 61, B-5000 Namur, Belgium

R. R. Chance
Allied Corporation, Corporate Research Center, Morristown, New Jersey 07960
(Received 30 January 1984)

The effect of charge-transfer doping on the geometric and electronic structures of conjugated polymers has been investigated at the *ab initio* level with explicit consideration of the doping agents. Three systems were chosen for study as prototypical examples of conjugated polymers with nondegenerate ground states: polyparaphenylene, polypyrrole, and polythiophene. As a result of charge transfer with electron-donating dopants, extra charges appear on the polymer chains and induce strong geometry modifications. The lattice evolves from an aromatic structure towards a quinoid-like structure. Charged defects associated with lattice deformations such as spinless bipolarons are formed. The influence on the electronic structure of the polymer chains is such that with respect to the undoped case, new states appear within the gap. For the maximum doping levels experimentally achieved, band-structure calculations demonstrate that the states in the gap overlap to form bipolaron bands, a few tenths of an electron volt wide. The presence of these bipolaron bands is consistent with optical data as well as with magnetic data which suggest that the charge carriers in the highly conducting regime are spinless.

I. INTRODUCTION

In recent years, the discovery of doped organic polymers with high conductivities has generated substantial research interest among physicists and chemists alike. On one hand, the creation of new materials combining the processability, light weight, and durability of plastics with the electrical conductivity of metals is a driving force in the development of conducting polymers. On the other hand, doped organic polymers constitute a new fascinating area of condensed-matter physics where nonlinear phenomena can play an important role. Polymers with doped derivatives reported to have conductivities larger than 1 S/cm include conjugated systems such as polyacetylene, polypyrrole, polythiophene, polyparaphenylene, and polyphenylene chalcogenides.[1,2] The doping process involves exposure of the polymer to electron donors (such as alkali metals) or acceptors (such as I_2 or AsF_5).

Although doped polymers display phenomena in some ways similar to conventional doped inorganic semiconductors, their physics is very different. One of the fundamental reasons for this difference is that these polymers are organic materials. Therefore, it is expected that charge-transfer (or electron-excitation) processes result in significant local modifications (relaxations) of the chain geometry. Indeed, in organic systems, the equilibrium geometry in the ionized (or excited) state is usually quite different from that in the ground state. In solid-state physics terminology, this means the electron-phonon coupling is strong. Furthermore, the local geometry modifications of the chain, in turn, markedly affect the electronic structure by inducing localized electronic states in the gap. These levels are all attributable to charge-transfer-induced modifications of the π system of the polymer and in that sense are intrinsic to the parent material, i.e., the organic polymer. Note that this is in contrast to the situation in doped inorganic semiconductors where the states in the gap are dopant levels. The fact that, upon ionization or electronic excitation, a local relaxation of the lattice geometric and electronic structures is energetically favorable, constitutes the basis of the fascinating physics occurring in doped organic polymers.

In order to understand the insulator-conductor transition in conjugated polymers in depth, it is very important to develop a detailed understanding of the modifications in geometry, as well as electronic structure, that are induced by the doping process. In this context, quantum-chemical *ab initio* techniques are well suited since they are known to produce high-quality ground-state geometries and properties of polymers.[3]

Thus far, polyacetylene (PA) has been the focus of most experimental and theoretical work. The reason is that the infinite chain of all-trans PA is unique among studied systems in possessing a degenerate ground state, i.e., two geometric structures having exactly the same total energy.

This degeneracy is a consequence of a Peierls distortion and leads to possible nonlinear soliton excitations and related structural deformations.[4,5] Many peculiar phenomena that occur in *trans*-PA can be explained by the presence of soliton defects on the chains. One of the most ex-

citing examples is the observation, with doping levels between about 0.2 and 7 mol % in AsF_5- (Ref. 6) and Na-doped PA,[7] of high conductivity without significant Pauli susceptibility. This has been considered as evidence that highly mobile spinless charged solitons are the charge carriers in that regime.

In other polymers, such as polyparaphenylene (PPP), polypyrrole (PPy), or polythiophene (PT), the ground state is nondegenerate. As a result, soliton excitations are not possible. However, doping of these polymers yields transport properties which are very similar to those of *trans*-PA. In particular, unusually low Pauli susceptibility has also been reported in the metallic regime of SbF_5-doped PPP,[8] and no ESR signal is detected in electrochemically cycled highly conducting PPy.[9] Recent theoretical[10–14] and experimental[9,15] work points to the evidence that bipolarons, i.e., doubly charged defects associated with a lattice deformation, are the corresponding spinless charge carriers in these systems.

In this paper, we focus on polymers with a nondegenerate ground state. We present a restricted Hartree-Fock (RHF) self-consistent-field (SCF) *ab initio* study of the geometries of polyparaphenylene, polypyrrole, and polythiophene in the undoped state and in the highly-Li-doped or highly-Na-doped state where bipolarons are likely to be present on the chains. We also examine, through valence effective Hamiltonian (VEH) calculations, the evolution of the electronic band structures upon doping of these compounds. Section II is devoted to a brief description of the methodology we have followed. In Sec. III we discuss the results of the SCF *ab initio* and VEH calculations on PPP, PPy, and PT. Conclusions of this work are presented in Sec. IV. Two preliminary reports of this work have been recently published and dealt with highly-Li-doped PPP and highly-Na-doped PPy.[16,17]

II. METHODOLOGY

The calculations on the geometry of undoped and highly doped polymer chains are performed in the framework of the RHF SCF–LCAO-MO (linear combination of atomic orbitals–molecular orbitals) *ab initio* technique.[18] All core and valence electrons are explicitly taken into account. We make use of the GAUSSIAN-76 program[19] as adapted and extended by one of us (J.G.F.) to handle 175 atomic orbitals on the 36-bit (binary digit) Digital Equipment Corporation DEC-20/60 computer of the Facultés Universitaires de Namur. All two-electron integrals smaller than 10^{-6} a.u. ($<2.721\times10^{-5}$ eV) are neglected. The convergence criterion required for each of the density matrix elements is 5×10^{-5} a.u. The symmetry of the compound can be explicitly taken into account in order to reduce the number of two-electron integrals to be evaluated.

We consider a minimal Slater-type-orbital–three-Gaussian (STO-3G) basis set where each atomic orbital ($1s$ for hydrogen; $1s$, $2s$, and $2p_{x,y,z}$ for carbon and nitrogen; $1s$, $2s$, $2p_{x,y,z}$, $3s$, and $3p_{x,y,z}$ for sulfur) is represented as a linear combination of three Gaussian functions. Standard molecularly optimized Slater exponents are used for these atoms.

In order to keep computing times at a reasonable level, the geometries are investigated on limited model chains: quaterphenyl (QP) for PPP, quaterpyrrole (QPy) for PPy, and quaterthiophene (QT) for PT. As dopant agents, we have chosen to take small alkali-metal atoms such as lithium or sodium. As a result, only the effects of *n*-type doping are explicitly examined. For lithium and sodium, we adopt a basis set which has been tested in calculations on cation-ligand interactions at the STO-3G level.[20] In the case of lithium, the $1s$ atomic orbital with exponent $\zeta=2.69$ is represented by six Gaussians (6G expansion); the $2s$ orbital, represented by a 3G expansion, has an optimized exponent $\zeta=0.95$; and the $2p$ orbitals are suppressed. In the case of sodium, a 3G expansion is used for all atomic orbitals; the exponents are taken to be $\zeta_{1s}=10.61$, $\zeta_{2sp}=3.48$, and $\zeta_{3s}=1.75$; and the $3p$ orbitals are suppressed.

In all calculations, the carbon–hydrogen and nitrogen–hydrogen bond lengths are kept at standard values, i.e., respectively, 1.08 and 0.99 Å. For undoped QP, we optimize seven parameters under D_2 symmetry: the torsion angle between two consecutive rings, the C–C bond between rings and within rings, the C–C bonds parallel to the chain axis and the bonds inclined with respect to it, the bond angles between an inclined bond, and, respectively, another inclined bond, a parallel bond, and a C–H bond. For the pyrrole and thiophene chains, *ab initio* calculations on the dimers have indicated that the most stable conformation corresponds to a situation where the rings are coplanar and alternate in such a way that nitrogen or sulfur atoms on adjacent rings point in opposite directions.[21] This is in agreement with the solid-state conformations as obtained from x-ray diffraction experiments for bipyrrole and terpyrrole,[22] and for bithiophene.[23] Therefore, for undoped QPy and QT, we consider the chains planar and optimize eight parameters under C_{2h} symmetry: the bond between rings and within rings, the C_α–N bond, the C_α–C_β bond, and the C_β–C_β bond, the C_α–N–C_α angle, the N–C_α–C_β angle, the C_α–C_β–C_α angle, and the N–C_α–C_α angle.

In the doped case, we add two lithium or sodium atoms to the tetramer. This corresponds to a very high doping level of 50 mol % on a per monomer basis. Each dopant is located above the middle of an inner ring. This choice allows measuring the extent of the influence of the dopant atoms by distinguishing between the inner and outer rings. We optimize the same parameters as in the undoped case, now under C_2 symmetry, and allow for different geometric relaxations in the inner and outer rings. The exact location of the dopant atoms is also optimized in the case of QPy and QT. For QP, in order to keep computation times low, the dopant is fixed at 1.85 Å above the middle of an inner ring, in analogy to what is found in the lithium-intercalated graphite compound.[24]

We may note that a STO-3G calculation for a single point on the potential hypersurface constructed to optimize the geometry requires about 2.5–3.5 h of CPU (central processing unit) time on the DEC-20/60 computer for QPy, QT, and undoped QP, and about 7 h of CPU time

for doped QP.

The optical transition energies are usually found to have little quantitative meaning at the RHF *ab initio* level. Therefore, in order to obtain the band-structure evolution for the chains upon doping, we have also performed VEH calculations.[25] We take the STO-3G geometries optimized on the undoped and highly doped tetramers as input geometries for the VEH calculations. The VEH technique has been shown to yield good values for band gaps and bandwidths in hydrocarbon,[26] sulfur-containing,[27] and nitrogen-containing[28] conjugated polymers.

III. RESULTS AND DISCUSSION

A. Polyparaphenylene

Among conducting polymer systems, polyparaphenylene is attractive for several reasons. High conductivities can be achieved, e.g., of the order of 500 S/cm upon AsF_5 doping and 30 S/cm upon potassium doping.[29] Formation of rechargeable batteries based on *n*-type-doped and *p*-type-doped PPP has been demonstrated.[30] AsF_5 doping of PPP oligomer single crystals (terphenyl, quaterphenyl, and sexiphenyl) provides a new solid-state polymerization process and also leads to highly conducting complexes.[31] Unlike polyacetylene, PPP is stable in air even at elevated temperatures.

PPP consists of benzene rings linked in the para position. Crystallographic data on oligomers[32–34] indicate that carbon–carbon bond lengths within the rings are about 1.40 Å and those between rings are about 1.51 Å. In the solid state, two successive benzene rings are tilted with respect to each other by about 23°. This torsion angle constitutes a compromise between the effect of conjugation and crystal-packing energy, which favor a planar structure, and the steric repulsion between hydrogen atoms in ortho positions, which favors a nonplanar structure. The band gap in PPP is 3.4 eV,[31] i.e., about twice that of polyacetylene.

The resonance form which can be derived for PPP corresponds to a quinoid structure.

Contrary to the situation in *trans*-polyacetylene, the benzenoid and quinoid forms are not energetically equivalent, the quinoid structure being substantially higher in energy. By performing STO-3G *ab initio* calculations on both conformations for quaterphenyl, we obtain an estimate of the energy difference between the benzenoid and quinoid forms of the order of 20.1 kcal/mol per ring.

1. Undoped chain

The STO-3G optimized geometry for quaterphenyl and the charges on carbon atoms as obtained from a Mulliken population analysis are displayed in Fig. 1. These optimized bond lengths and bond angles are in close agreement with x-ray and neutron diffraction data on terphenyl and

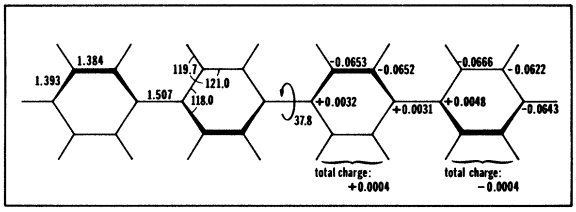

FIG. 1. STO-3G–optimized geometry (bond lengths in Å and angles in deg) and net charges on carbon atoms (in $|e|$) for quaterphenyl, assuming D_2 symmetry.

quaterphenyl. The slight quinoid structure that is obtained within the rings is supported by the neutron diffraction results on terphenyl.[33] Though significantly larger than the solid-state value, the 37.8° torsion angle agrees well with the 42° estimate from diffraction data on gaseous biphenyl.[35] It is interesting to note that the maximum difference in C–C bond length is 0.123 Å, in close agreement with experiment. This is larger than the 0.08-Å estimate for *trans*-PA.[36] Charges on carbon atoms connected to hydrogen atoms are of the order of 0.06*e*, due to the slight polarization of the C–H bond. Total charges per CH unit are however negligibly small.

We have performed VEH calculations on quaterphenyl and polyparaphenylene using the STO-3G coordinates optimized on undoped QP, except for the torsion angle which is set at the 22.7° solid-state value. We obtain band-gap values of 4.3 and 3.5 eV, respectively, for QP and PPP. This compares very well with the experimental data: 4.5 eV for terphenyl, 3.9 eV for sexiphenyl, and 3.4 eV for PPP.[31]

2. Doped chain

We have considered both the lithium and sodium doping of quaterphenyl. Both these alkali metals are known to yield highly conducting complexes with PPP.[29] In the lithium-doped case, the charge transfer towards the chain is calculated to be 0.64*e* per lithium atom; see Fig. 2. We find from the total charge per ring that most of the charge is transferred to the inner rings, only 22.5% going

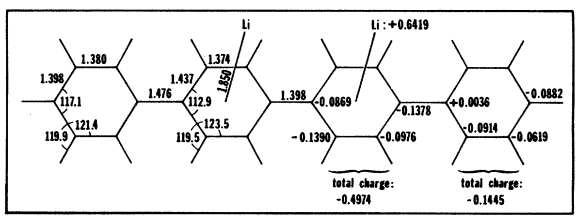

FIG. 2. STO-3G–optimized geometry (bond lengths in Å and angles in deg) and net charges on lithium and carbon atoms (in $|e|$) for lithium-doped quaterphenyl, assuming C_2 symmetry. Optimized torsion angle between two consecutive rings is 2.0°.

to the outer rings. Although end effects may not be neglected, this indicates that in longer chains the charge transferred to (and the influence of the dopant on) next-nearest-neighbor rings should be fairly small. Since these calculations take into account the charge transfer from two dopant atoms, we are mimicking the situation where a doubly charged spatially localized defect (a bipolaron) is present on the chain. Our results thus suggest that bipolarons in PPP would mainly extend over about four rings. Hückel-like calculations predict a bipolaron width of the order of five phenyl rings.[13]

Charge transfer from the lithium atoms causes drastic modifications of QP geometry, as depicted in Fig. 2. The chain becomes nearly coplanar, the torsion angle changing from 37.8° to 2.0°. As a result of the difference in the amount of charge transfer between the inner and outer rings, the changes in the geometrical parameters are larger in the inner rings. In these rings, the C—C bond between rings is markedly reduced by 0.109 to 1.398 Å. Parallel bonds in the rings acquire a more pronounced double-bond character as they decrease by 0.010 Å. Inclined bonds increase significantly by 0.044 Å. The maximum C—C bond-length difference in the inner rings becomes 0.063 Å, i.e., half of the value found in the undoped case. These changes give the inner rings a strong quinoidal character. This result is in agreement with crystallographic data on biphenyl and biphenyl anions, indicating an increased admixture of the quinoid resonance form in the anions.[37] The same is true for the outer rings, to a smaller extent, however; bonds within rings change by less than 0.005 Å and bonds between rings decrease by 0.031 Å.

In the case of sodium doping, the charge transfer is almost complete, 0.93e per Na atom. The geometry and net charges per sodium and carbon atom are given in Fig. 3. As for Li doping, about 80% of the charge goes to the inner rings. The chain is now completely coplanar. The inner rings are almost purely quinoid with 1.352-Å and 1.371-Å double bonds and 1.462-Å single bonds. It is interesting to note that the maximum C—C bond-length difference is 0.110 Å, i.e., significantly larger than in the lithium-doped case.

The influence of the geometric modifications on the electronic structure of the chain is very important. With respect to the undoped case, the level corresponding to the highest occupied molecular orbital (HOMO) is strongly pushed up in energy, whereas the level corresponding to the lowest unoccupied molecular orbital (LUMO) is strongly pushed down in energy. All the other levels remain more or less at the same energies as in the undoped compound. This is illustrated in Table I where we present the evolution, at the VEH level, from the undoped situation (torsion angle set at 22.7°) to the sodium-doped situation for the QP highest occupied and lowest unoccupied π levels. The VEH calculations on QP indicate that, in comparison to the undoped molecule, the upward shift of the HOMO and the downward shift of the LUMO are, respectively, 0.50 and 0.62 eV upon lithium doping and 0.74 and 0.88 eV upon sodium doping. The shifts are larger in the latter case since the geometric modifications are larger.

We thus observe the *appearance of two states in the gap* due to the charge transfer and the geometry changes implied by the formation of a doubly charged bipolaron defect on the chain. These states in the gap can then be referred to as bipolaron states and are fully occupied in the case of n-type doping as we consider here. They would be empty in the case of p-type doping. Thus the bipolarons are spinless. The STO-3G calculations show that the bipolaron states are dominated by the C π orbitals (fairly small contributions from Li 2s orbitals are present in the Li-doped case). The impurity states (that is, those related to the dopant atoms) appear above the bipolaron states. For the lithium doping, the impurity states correspond to mixtures of Li 2s and C π orbitals and are located between the highest bipolaron state and the QP conduction levels. The Na 3s impurity states appear within the conduction states and not within the gap.

It should be stressed that the calculations presented for the doped cases correspond to very high doping levels. As discussed previously at the Hückel level, at low dopant concentrations polarons (singly charged defects corresponding to radical ions and carrying spin) are expected to be present on the chains rather than bipolarons.[10,13] However, two adjacent polarons are predicted to recombine to form a bipolaron.[10,13] Within Hückel theory, with consideration of neither Coulomb repulsion or screening due to the counterions, the formation of a bipolaron is favored

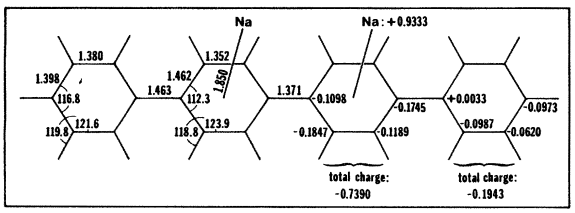

FIG. 3. STO-3G—optimized geometry (bond lengths in Å and angles in deg) and net charges on sodium and carbon atoms (in $|e|$) for sodium-doped quaterphenyl, assuming C_2 symmetry. Optimized torsion angle between two consecutive rings is 0.0°.

TABLE I. VEH energies (in a.u.) for the highest occupied and lowest unoccupied π levels in quaterphenyl and sodium-doped quaterphenyl. Note that 1 a.u. of energy is equal to 27.21 eV.

Undoped	Sodium doped
−0.1348 (LUMO)	−0.1669
−0.2916 (HOMO)	−0.2644
−0.3225	−0.3199
−0.3440	−0.3460
−0.3449	−0.3461
−0.3458	−0.3538
−0.3465	−0.3559
−0.3599	−0.3594

over that of two polarons by about 0.36 eV.[10,13]

Having this in mind, we can draw the following picture for the evolution of the PPP band structure upon sodium doping. For the undoped PPP chain, the band gap of 3.5 eV [Fig. 4(a)]. At high doping levels, bipolarons are formed either directly or as a result of recombinations among polarons. Bipolaron states appear in the gap, 0.74 eV above the valence-band (VB) edge and 0.88 eV below the conduction-band (CB) edge [Fig. 4(b)]. As the doping level increases, bipolaron states start overlapping and this process leads to the formation of bipolaron bands within the gap. Taking as input geometry that of sodium-doped QP, we have performed a VEH band-structure calculation for a chain with a 50-mol % doping level, which corresponds to the maximum concentration usually achieved experimentally. The resulting band structure is sketched in Fig. 4(c). It shows that two bipolaron bands are present in the gap and have widths of 0.55 eV.

Upon application of an electric field, the possible motion of the doubly charged bipolarons along the chains and between the chains leads to a conduction mechanism without spin. This conduction mechanism is very unusual since all bands, as can be observed from Fig. 4(c), are either totally full or empty. (Note that an investigation of possible bipolaron interchain transport has been presented elsewhere.[38]) This spinless conductivity mechanism is consistent with the absence of any significant Pauli susceptibility in the metallic regime of SbF_5-doped PPP.[8] Furthermore, the band structure of Fig. 4(c) is in agreement with electron-energy-loss spectra for AsF_5-doped PPP.[39] Those spectra indicate the appearance upon p-type doping of two peaks near about 1 eV and near about 2 eV, corresponding to transitions from the valence band to two relatively narrow bands in the gap. The lower-energy peak is much more intense, as is predicted by optical-absorption calculations on bipolarons using a continuum-coupled electron-phonon Hamiltonian generalized to model unique ground-state situations as in PPP.[40]

If we consider a hypothetical doping level of 100 mol % (one dopant per monomer), as is the case for the band structure displayed in Fig. 4(d), we obtain a merging of the lower (higher) bipolaron band with the VB (CB). Traditional conductivity with spin could then occur due to the partially filled character of the CB (VB) upon n-(p-) type doping. There remains a gap of about 1 eV between the original VB and CB. This contrasts with the situation in highly doped PA where the original gap is believed to vanish.[41]

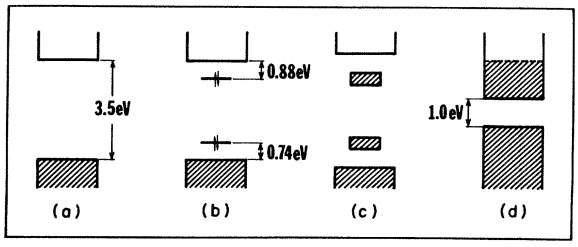

FIG. 4. Evolution of the VEH band structure of polyparaphenylene upon sodium doping: (a) undoped, (b) intermediate doping level with bipolaron states present in the gap, (c) 50-mol % doping level, formation of bipolaron bands, and (d) hypothetical 100-mol % doping level.

In order to illustrate more precisely the evolution of the band structure as a function of doping-induced geometry modifications, we present in Fig. 5 the VEH π band structure for (a) a PPP chain having the STO-3G geometry of undoped QP, (b) a polyquaterphenyl chain with the STO-3G geometry of sodium-doped QP, and (c) a polyquinoid chain having the geometry of an inner ring from sodium-doped QP. Situations (a), (b), and (c) can thus be viewed as corresponding respectively to 0, 50, and 100 mol % doping levels. Note that, since the unit cell for the polyquaterphenyl chain is 4 times as large as that for the PPP and polyquinoid chains, there are 4 times as many π bands in the band structure of Fig. 5(b).

In case (a) we obtain the usual PPP π band structure which has been discussed in detail, e.g., in Ref. 42. The band gap is 3.5 eV. In case (b) we clearly see the appearance of the two bipolaron bands in the gap. Since the lower bipolaron band comes out of the VB and the higher one out of the CB, the band gap between the VB edge (band $\pi 3c$) and the CB edge (band $\pi 4b$) increases to 4.5 eV. In case (c) the bipolaron bands are incorporated back into the VB and CB and the gap between bands $\pi 3$ and $\pi 4$ decreases to 1.0 eV.

It is interesting to note that for a polyquinoid chain having the STO-3G geometry of the inner rings from lithium-doped QP, the gap between bands $\pi 3$ and $\pi 4$ is 1.7 eV. This is larger than for the sodium-doped structure, although the maximum difference in C—C bond length is much smaller as previously mentioned (0.063 vs 0.110 Å). This contrasts to the situation in polyacetylene where the gap increases with an increasing difference in C—C bond lengths.

As we can observe from Fig. 5, the quinoid structure has a lower ionization potential and a larger electron affinity than the benzenoid structure (and, as a result, a smaller band gap). This explains that upon doping the presence of an extra charge on the chain induces a local geometry relaxation from the benzenoid structure towards the quinoid structure. Thus the formation of a charged defect such as a bipolaron actually occurs when the lowering in ionization energy due to the presence of a quinoid segment more than compensates for the increase in elastic energy required to form that quinoid segment.

B. Polypyrrole

Polypyrrole has attracted a great deal of attention in the past years.[43–45] Conducting polypyrrole films can readily be obtained by oxidative electrochemical polymerization of pyrrole monomer.[46] Conductivities ranging between 10 and 100 S/cm are typically obtained. The conducting oxidized films have good mechanical properties and display much better environmental stability that the other conducting polymers such as doped polyacetylene or polyparaphenylene. The films usually consist of cationic PPy polymer and ClO_4^- or BF_4^- anions. The ratio of

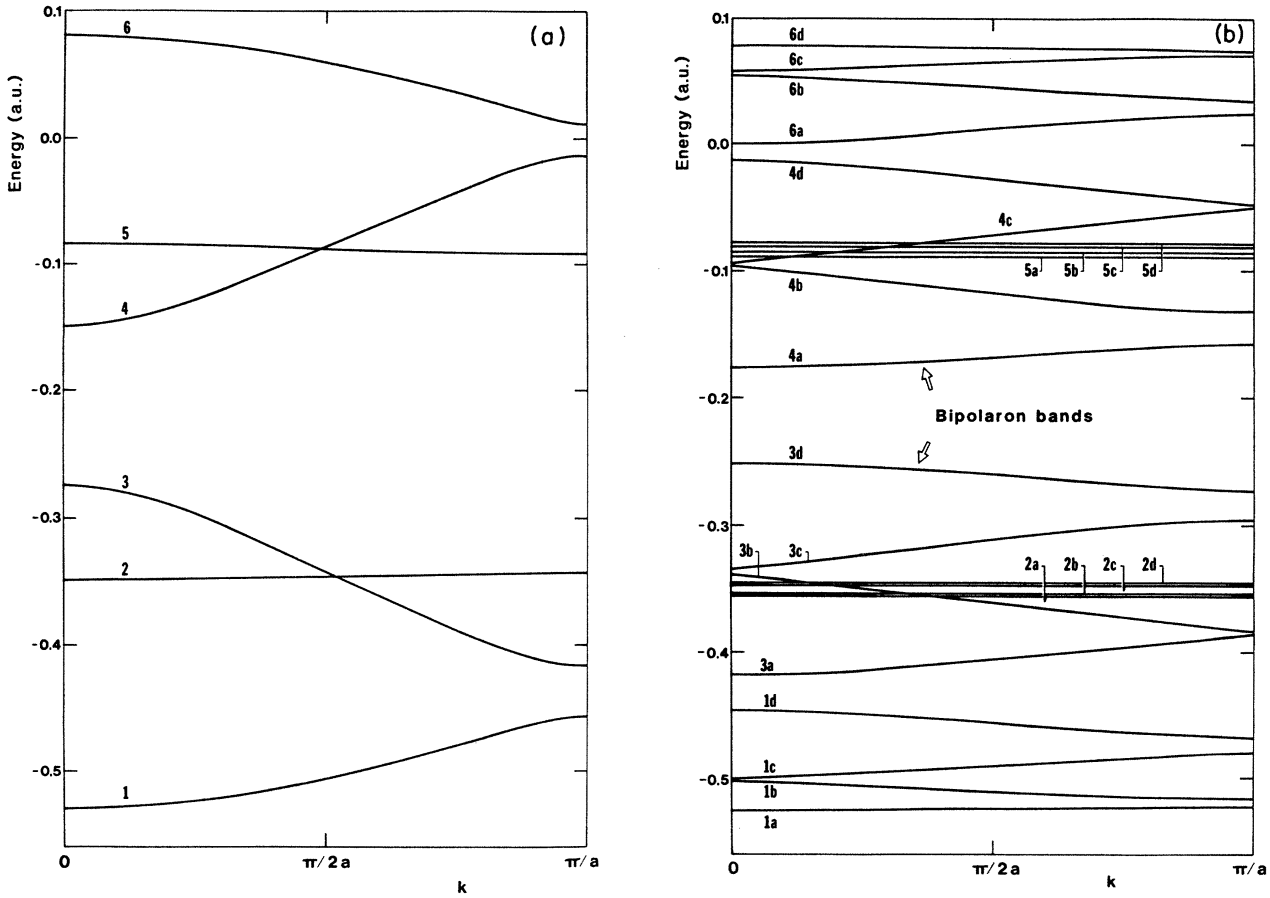

FIG. 5. VEH π band structure for (a) a polyparaphenylene chain, with STO-3G geometry from undoped quaterphenyl corresponding to 0-mol % doping level, (b) a polyquaterphenyl chain, with STO-3G geometry from sodium-doped quaterphenyl corresponding to 50-mol % doping level, and (c) a polyquinoid chain, with STO-3G geometry from an inner ring of sodium-doped quaterphenyl corresponding to a 100-mol % doping level.

pyrrole units to anions is of the order of 3 to 1 in the as-grown films.

As previously mentioned, recent x-ray data on small PPy oligomers (bipyrrole and terpyrrole[22]) indicate that the rings are coplanar and that adjacent rings are connected at the α position [which is consistent with ^{13}C NMR data on PPy (Ref. 43)] and alternate such that the nitrogen atoms point in opposite directions.

A resonance form can be derived for PPy that corresponds along the carbon path to a cis-polyacetylene cis-transoid structure.

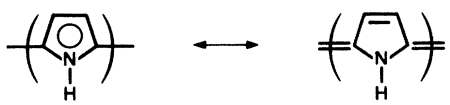

For sake of simplicity, we will refer to this resonance form as the quinoid form. As for PPP, the two resonance forms in PPy are not energetically equivalent. From STO-3G calculations on both forms in quaterpyrrole, we find that the aromatic form is more stable by 14.4 kcal/mol per ring. With respect to PPP, the stability difference at the STO-3G level for PPy appears a bit smaller.

Owing to computational limitations, we are forced to consider n-type doping with alkali-metal atoms, although no such doping has ever been experimentally successful to date on polypyrrole. It must be borne in mind, however, that the presence of alkali-metal atoms in our calculations has to be understood as a convenient way to investigate the influence of extra charges on the chains while taking counterions explicitly into account. The possible differences in the effects of n-type and p-type doping will be discussed.

1. Undoped chain

The STO-3G optimized geometry for quaterpyrrole is presented in Fig. 6 together with the charges on carbon and nitrogen atoms. Note that nitrogen is a strong π donor ($-0.35e$), but an even stronger σ acceptor ($0.66e$), so that it has a net charge of $0.31e$.

The bond lengths within rings are in excellent agreement with the experimental data.[22] For instance, the average values observed by x-ray diffraction in the middle ring of terpyrrole are $r_{C\text{-}N}=1.388$ Å, $r_{C_\alpha\text{-}C_\beta}=1.360$ Å, and $r_{C_\beta\text{-}C_\beta}=1.412$ Å. The bond connecting rings is calculated larger (1.474 Å) than those within rings, but are, however, significantly smaller than the similar bond in PPP (1.507 Å). The experimental value is actually even shorter, of the order of 1.448 Å, implying that this bond

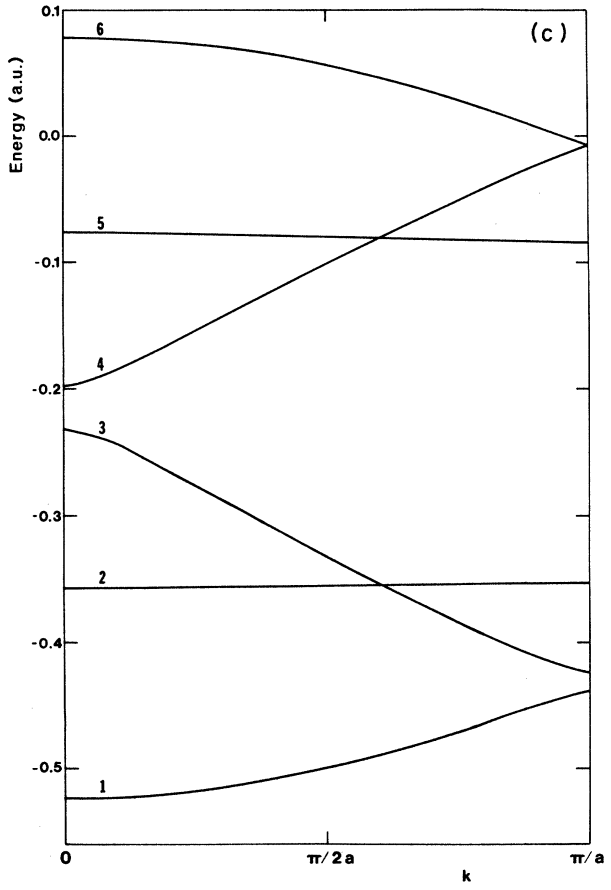

FIG. 5. (*Continued.*)

has some double-bond character. The maximum C—C or C—N bond-length difference is 0.111 Å, a bit smaller than in PPP (0.123 Å). Total net charges per ring are negligibly small.

VEH calculations on QPy and PPy chains having the STO-3G—optimized geometry result in first optical transition energies of, respectively, 4.8 and 4.0 eV. This band-gap value for PPy is in reasonable agreement with the 3.2-eV experimental estimate for neutral PPy.[43] The larger theoretical value can be explained, at least partly, by the longer inter-ring bond length that is considered with respect to the experimental value (see, for instance, Table I in Ref. 47: for a fixed ring geometry, the band gap is lowered from 4.0 to 3.6 eV when decreasing the inter-ring bond length from 1.49 to 1.45 Å).

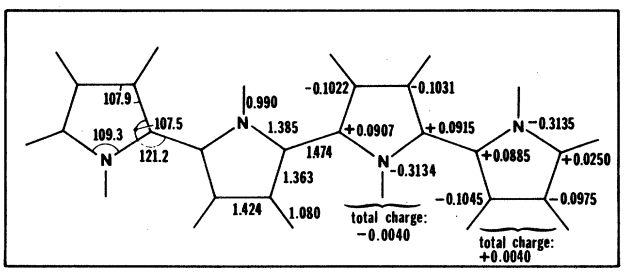

FIG. 6. STO-3G—optimized geometry (bond lengths in Å and angles in deg) and net charges on carbon and nitrogen atoms (in | *e* |) for quaterpyrrole, assuming C_{2h} symmetry.

2. *Doped chain*

We have investigated both lithium and sodium doping. In the lithium case, contrary to what occurs for PPP, almost no charge transfer is obtained. This reflects the lower electron affinity of PPy relative to PPP. VEH calculations indicate that the electron affinity of PPy is about 1.5 eV smaller than that of PPP and about 2.5 eV smaller than those of PA and PT.[47]

Similar to our results for sodium-doped QP, the charge transfer in sodium-doped QPy is predicted to be almost complete (0.94*e* per sodium atom) and the charge goes predominantly to the inner rings, only 23% being transferred to the outer rings. The optimized geometry of Na-doped QPy is presented in Fig. 7. The sodium atoms are found 1.98 Å above the plane of an inner ring at 2.25 Å from the nitrogen and about 2.33 Å from the carbons. The geometric modifications in the inner rings are such that along the carbon path, the C—C singlelike bonds and doublelike bonds are interchanged with respect to the undoped case: the C_β—C_β bond decreases by 0.044 Å to 1.380 Å, and the C_α—C_β bond increases from 1.363 Å up to 1.437 Å. The bond connecting rings goes down by 0.117 Å to 1.357 Å. The C—N bonds elongate by 0.043 Å to 1.428 Å. The maximum C—C or C—N bond-length difference in the inner rings is 0.080 Å. The modifications in the outer rings are quite weaker than in the quaterphenyl case, suggesting that the width of a bipola-

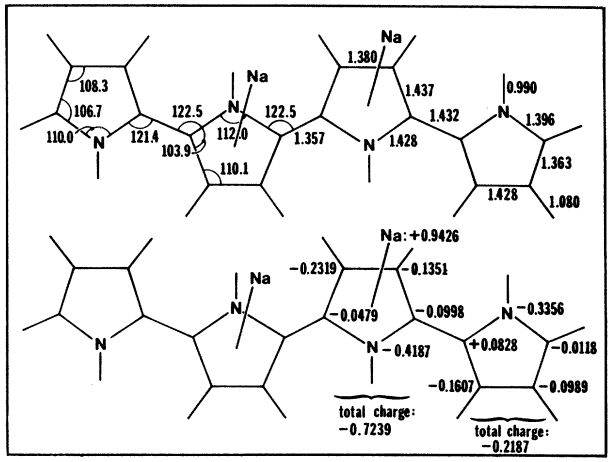

FIG. 7. STO-3G—optimized geometry (bond lengths in Å and angles in deg) and net charges on sodium, nitrogen, and carbon atoms (in | *e* |) for sodium-doped quaterpyrrole, assuming C_2 symmetry.

ron defect could be smaller in a polypyrrole chain than in a polyparaphenylene chain.

It is very important to point out that an analysis of the frontier orbitals tends to indicate that *upon p-type doping, the geometry changes along the carbon path should be very similar,* whereas the elongation of C—N bond could be smaller. The conclusions drawn from these sodium-doped calculations should therefore be fully applicable to the *p*-type—doping process.

As in PPP chains, the influence of the geometric modifications on the electronic structure is such that, in comparison to the undoped case, two (bipolaron) states appear in the gap: the HOMO level is pushed up in energy and the LUMO level is pushed down; the other levels move much less. The evolution upon doping of the highest occupied and lowest unoccupied π levels in QPy is given in Table II. In marked contrast to PPP systems, however, the shifts of the HOMO and LUMO levels are very different. The VEH calculations on QPy show that the HOMO upward shift is of the order of 0.60 eV, whereas the LUMO downward shift is about 1.08 eV.

Previously, we have argued[17] that this asymmetry in the locations of the bipolaron states with respect to the gap center could be explained by the fact that the atomic-orbital contributions to undoped QPy or PPy HOMO and LUMO levels are quite different. Indeed, the HOMO level has, for symmetry reasons, no contributions from the nitrogen π orbitals and is thus equivalent to the *cis*-PA HOMO level; the LUMO level has important contributions from all carbon and nitrogen π orbitals. This is illustrated in Fig. 8. However, as will be shown later, such a large asymmetric shift is not observed in polythiophene, which has HOMO and LUMO wave functions almost identical to those in PPy, thereby weakening our argument for PPy.

The VEH band-structure evolution of polypyrrole upon sodium doping is presented in Fig. 9. As noted earlier, for undoped PPy, we obtain a band gap of 4.0 eV [Fig. 9(a)]. At low doping levels, in analogy to the PPP situation, Hückel-like calculations predict that polarons are formed on the PPy chains.[14] At intermediate doping levels, interactions between polarons lead to the formation of bipolarons, a bipolaron being 0.45 eV more stable than two polarons.[14] This picture is supported by available ESR (Ref. 9) and optical[14] data. Bipolaron states then appear in the

TABLE II. VEH energies (in a.u.) for the highest occupied and lowest unoccupied π levels in quaterpyrrole and sodium-doped quaterpyrrole.

Undoped	Sodium doped
−0.0621 (LUMO)	−0.1017
−0.2381 (HOMO)	−0.2161
−0.2813	−0.2842
−0.3334	−0.3353
−0.3494	−0.3497
−0.3506	−0.3504
−0.3507	−0.3572
−0.3524	−0.3591

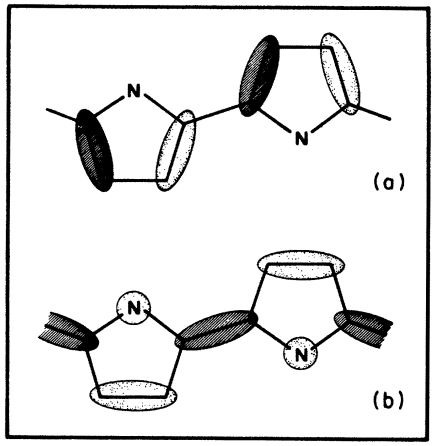

FIG. 8. Schematic representation of the LCAO π coefficients at $k=0$ for the (a) HOMO and (b) LUMO in polypyrrole, illustrating the regions of electronic concentration.

gap and, as mentioned above, are calculated at the VEH level to be located 0.60 eV above the VB edge and 1.08 eV below the CB edge [Fig. 9(b)].

We have performed a VEH band-structure calculation on a PPy chain whose geometry corresponds to a per monomer 33-mol % doping level (six rings form the polymer unit cell: two of them have the geometry of undoped QPy, and the remaining four have the geometry of Na-doped QPy). This is the acceptor dopant concentration which is usually achieved in the films grown upon electrochemical polymerization in $AgClO_4$ electrolyte.[43] The band structure is sketched in Fig. 9(c) and detailed in Fig. 10. We observe the presence of two bipolaron bands in the gap. These bands have widths of 0.24 and 0.10 eV. They are narrower than in the corresponding PPP case. This can be explained by the fact that the maximum dop-

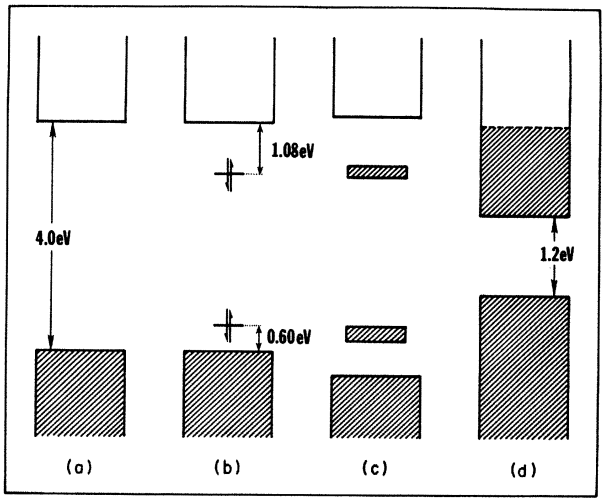

FIG. 9. Evolution of the VEH band structure of polypyrrole on sodium doping: (a) undoped, (b) intermediate doping level with bipolaron states present in the gap, (c) 33-mol % doping level, formation of bipolaron bands, and (d) hypothetical 100-mol % doping level.

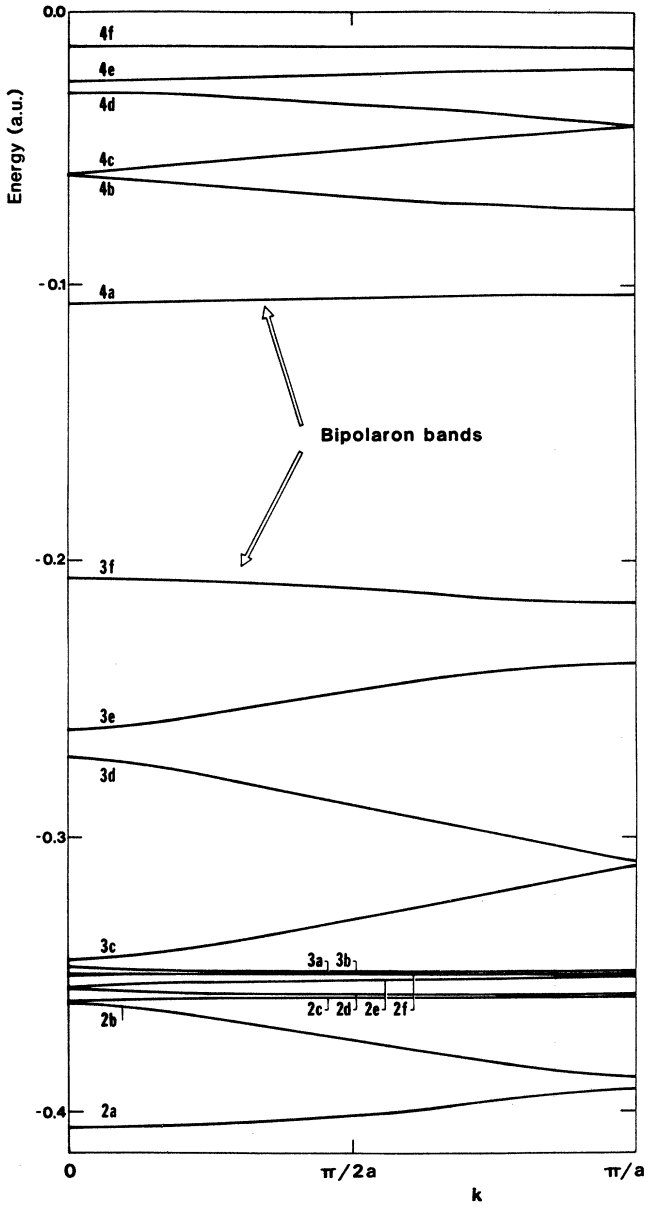

FIG. 10. VEH π band structure for a polyhexapyrrole chain. The first four rings of the unit cell have the STO-3G geometry from sodium-doped quaterpyrrole and the remaining two rings have that of undoped quaterpyrrole.

ing level in PPy (33 mol %) is lower than that in PPP (50 mol %), and the PPy bipolaron width seems smaller. We may add that in the Hückel-like calculations (which use the STO-3G geometries calculated in this work and where parameters are optimized to reproduce the optical spectrum of the undoped chain), the widths of the bipolaron bands are significantly larger, of the order of 0.4 eV.[14]

The presence of those two bipolaron bands is consistent with the appearance of two absorption bands within the gap in the optical spectrum of as-grown PPy films. The VB-to-CB transition is calculated to increase by 0.5 eV with respect to the undoped case; experimentally, the increase is of the order of 0.4 eV. A conductivity mechanism based on the motion of bipolarons is consistent with the absence of ESR signal in electrochemically cycled, highly conducting PPy.[9]

If higher doping is considered such as one dopant per pyrrole unit [Fig. 9(d)], VEH calculations predict, as for PPP, the merging of the lower bipolaron band with the VB and the higher one with the CB. Conductivity with spin could then occur. The original 4.0-eV band gap does not close, but decreases to 1.2 eV as a result of a 1.1-eV upward shift of the VB edge and 1.7-eV downward shift of the CB edge.

C. Polythiophene

Polythiophene [poly(2,5-thienylene)] can be chemically synthesized from dihalogenated thiophene by utilizing a dehalogenation polymerization.[48–50] The chemical synthesis leads to a fairly well-ordered (about 50% crystalline) material which is reported to be indefinitely stable in air at room temperature and thermally stable under nitrogen atmosphere up to 400 °C.[50] Degrees of polymerization of about 50 monomer units are obtained.[50] Doping of chemically prepared PT with 24 mol % AsF_5 leads to a room-temperature conductivity of about 14 S/cm.[50] Polythiophene can also be electrochemically synthesized,[51–53] much in the same way as polypyrrole, to produce a more disordered material. Conductivities for electrochemically prepared PT with one BF_4^- anion per three thiophene units range between 10 and 100 S/cm.

The quinoidlike resonance form which is derived for polythiophene is similar to that in PPv.

The stability difference between the aromatic and quinoid form is estimated, from STO-3G calculations on quaterthiophene, to be about 16.1 kcal/mol per ring. This is slightly larger than the difference in PPy (14.4 kcal/mol per ring) and smaller than in PPP (20.1 kcal/mol per ring).

To the best of our knowledge, no *n*-type doping of PT has been reported so far; *n*-type doping should, however, yield highly conducting complexes since the electron affinity of PT is estimated from VEH calculations to be comparable to polyacetylene or about 1 eV higher than in PPP.[47] We will only consider here the sodium doping of PT.

1. Undoped chain

The STO-3G geometry and the charges on carbon and sulfur atoms are displayed in Fig. 11. The sulfur atom within a thiophene ring is as good a π donor ($-0.24e$) as nitrogen in a pyrrole ring but is not a σ acceptor. As a result, the net charges on the sulfur atoms in quaterthiophene are positive ($-0.27e$) and those on α carbons are about $0.2e$ more negative than in QPy. This is, of course, related to the difference in electronegativity between nitrogen (3.0) and sulfur (2.5), the electronegativity of sulfur being essentially the same as that of carbon.

Within the rings of QT, the bond lengths along the *cis*-polyacetylene-like path show greater alternation than in

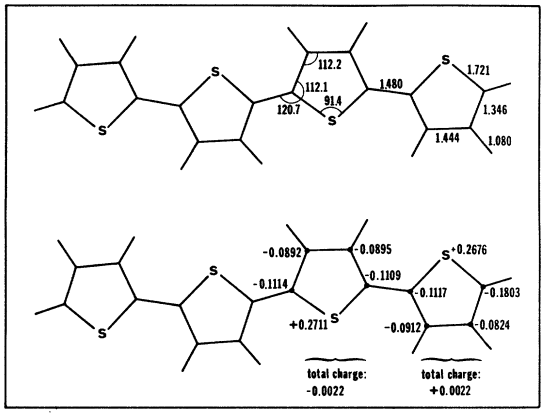

FIG. 11. STO-3G—optimized geometry (bond lengths in Å and angles in deg) and net charges on carbon and sulfur atoms (in $|e|$) for quaterthiophene, assuming C_{2h} symmetry.

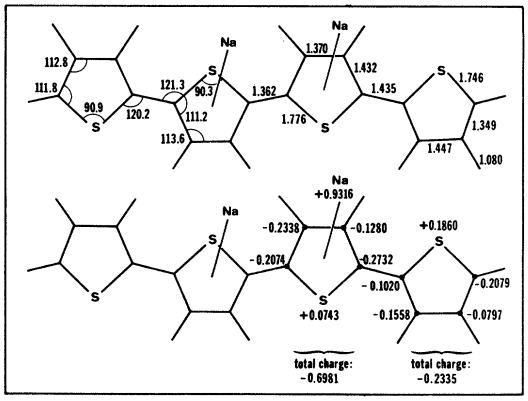

FIG. 12. STO-3G—optimized geometry (bond lengths in Å and angles in deg) and net charges on sodium, sulfur, and carbon atoms (in $|e|$) for sodium-doped quaterthiophene, assuming C_2 symmetry.

QPy (1.346 and 1.444 Å in QT vs 1.363 and 1.424 Å in QPy). The ring-connecting bond (1.480 Å) is slightly longer than in QPy by 0.006 Å. The maximum C—C bond-length difference is 0.134 Å, which is a bit larger than in both QP and QPy. As expected, total net charges per ring are very small.

It is quite difficult to compare our geometry results with the experimental data on bithiophene (2,2′-dithienyl) since the x-ray geometry is quite imprecise due to crystal decomposition upon irradiation.[23] Electron diffraction data are available on gaseous bithiophene[54] (which is, however, believed to be twisted) and indicate the following bond lengths: $r_{C\text{-}S}=1.717$ Å, $r_{C_\alpha\text{-}C_\beta}=1.357$ Å, and $r_{C_\beta\text{-}C_\beta}=1.433$ Å; the bond between rings is equal to 1.480 Å. The C—S—C angle is 92.0°. All these values are in good agreement with our optimized values. Note that a comparison of the microwave data on thiophene and pyrrole is consistent with a larger C—C bond alternation in thiophene with respect to pyrrole.[55]

VEH calculations have been performed on undoped QT and PT chains with the STO-3G optimized geometries. The first optical transition energies are calculated to be, respectively, 3.0 and 2.2 eV. This agrees very well with experimental values of the order of 3.2 eV for the absorption peak in QT) (Ref. 56) and 2.0 eV for the absorption edge in PT.[52,57,58] As in the case of PPy, the HOMO level has no contribution from the π atomic orbitals on the sulfur atoms.

2. Doped chain

Although polypyrrole and polythiophene might be expected to have very similar properties, the doping of these systems leads in some instances to quite different results, especially with regard to the band-structure evolution.

The STO-3G geometry and charges for sodium-doped PT are given in Fig. 12. The same charge transfer per sodium atom ($0.93e$) is found as for the QP and QPy compounds. The majority of the charge (75%) goes to the inner rings. The sodium atoms are optimized to be located 1.62 Å above the plane of the molecule, at 2.59 Å from the nearest sulfur atom, and about 2.4 Å from the carbons. They are thus closer to the carbons than the sulfur, in contrast to the situation in QPy. This can be explained by the fact that both the sodium and sulfur atoms have a net positive charge.

The geometry modifications in the inner rings provoke, along the carbon path, the interchange of the singlelike and doublelike bonds as compared to the undoped case. This is the same trend as in QPy. The bonds between rings decrease by 0.118 Å to 1.362 Å, the C_β—C_β bond decreases from 1.444 to 1.370 Å, and the C_α—C_β bond elongates by 0.086 Å to 1.432 Å. This means that the maximum C—C bond-length difference becomes 0.070 vs 0.080 Å in Na-doped QPy. The C—S bond undergoes a 0.055-Å increase to 1.776 Å. The modifications in the outer rings are much smaller and similar to those found in the outer rings of doped QPy.

The VEH evolution of the highest occupied and lowest unoccupied π levels from undoped to Na-doped QT is given in Table III. Upon doping, the HOMO undergoes an upward shift of 0.61 eV and the LUMO undergoes a downward shift of 0.71 eV. This contrasts to QPy where the (bipolaron) states come into the gap with a large asymmetry with respect to the gap center. The calculated shifts in PT are in excellent agreement with the optical-

TABLE III. VEH energies (in a.u.) for the highest occupied and lowest unoccupied π levels in quaterthiophene and sodium-doped quaterthiophene.

Undoped	Sodium doped
−0.1746 (LUMO)	−0.2008
−0.2844 (HOMO)	−0.2619
−0.3211	−0.3206
−0.3417	−0.3447
−0.3430	−0.3448
−0.3450	−0.3520
−0.3462	−0.3551
−0.3649	−0.3631

absorption data[58] which show the presence of two peaks within the gap located, respectively, about 0.60—0.65 eV above the VB edge and 0.65—0.70 eV below the CB edge.

The VEH evolution of the PT band structure upon doping is given in Fig. 13. The band gap in the undoped system is 2.2 eV [Fig. 13(a)]. (A detailed description of the VEH band structure for neutral PT has been presented in Ref. 27.) At intermediate (a few mol %) doping levels, by analogy with what is found in PPP and PPy, we consider the situation where bipolaron states appear in the gap, at 0.61 eV above the VB edge and 0.71 eV below the CB edge [Fig. 13(b)].

A VEH band-structure calculation has been performed for the 33-mol % doping level which corresponds to that achieved during the electrochemical polymerization [Fig. 13(c)]. The corresponding detailed π band structure is displayed in Fig. 14. The bipolaron states at such a high-dopant-concentration overlap and form two bands in the gap, 0.24 and 0.19 eV wide. The original band gap increases from 2.2 eV in the undoped state to 2.9 eV. Experimentally, as far as can be judged from Fig. 6 in Ref. 58, the band gap appears to increase by 0.4 eV for the 20-mol % doping level. The presence of these bipolaron bands in the gap explains the interesting electrochromic effect that is observed in PT.[57] By stepping the potential of the PT film between 0.0 and 1.0 V vs Ag/Ag^+, the film may be made to switch from red to green. The neutral film is red due to an absorption peaking at 2.6 eV, corresponding to the π-π^* transition. The oxidized film is green due to an absorption at about 1.7 eV which can be related to a transition from the VB to the upper bipolaron band upon p-type doping (or from the lower bipolaron band to the CB upon n-type doping). Magnetic measurements in the highly conducting regime of PT would be very desirable in order to assess whether spinless bipolarons can be the charge carriers, as would be suggested by our calculations.

For an hypothetical 100-mol % doping level, the VEH calculations indicate, as for PPP and PPy, that the lower (upper) bipolaron band merges with the VB (CB) [Fig. 13(d)]. However, the importance of the shifts for the states appearing in the gap upon doping, coupled with the small value of the original band gap, has the consequence that the gap between the VB and CB edges almost closes, our prediction being as small as 0.14 eV. This is consistent with both optical-absorption data indicating that the band gap disappears and thermopower data suggesting metalliclike behavior, for experimental doping levels larger than 20 mol %.[58] The discrepancy between the theoretical and experimental doping levels for which the closure occurs can be understood by the fact that a single-chain approach is used in our calculations.

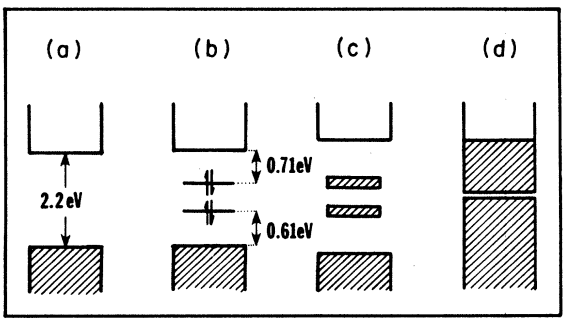

FIG. 13. Evolution of the VEH band structure of polythiophene on sodium doping: (a) undoped, (b) intermediate doping level with bipolaron states present in the gap, (c) 33-mol % doping level, formation of bipolaron bands, and (d) hypothetical 100-mol % doping level.

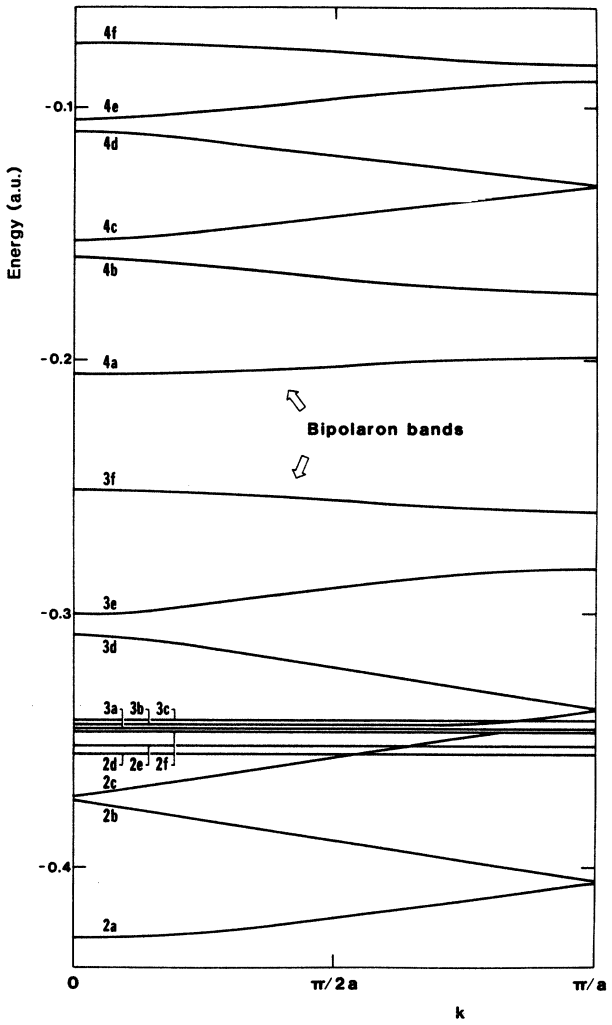

FIG. 14. VEH π band structure for a polyhexathiophene chain. The first four rings of the unit cell have the STO-3G geometry from sodium-doped quaterthiophene and the remaining two rings have that of undoped quaterthiophene.

IV. CONCLUSIONS

The three polymers we have investigated as being representative of conducting polymer systems with a nondegenerate ground state display a similar behavior upon doping. The presence of extra charges on the chains leads to the formation of charged defects such as spinless bipo-

larons associated with strong geometric modifications and the appearance of electronic states in the gap. For the maximum doping levels experimentally achieved, of the order of 50 mol % in polyparaphenylene and 33 mol % in polypyrrole and polythiophene, bipolaron bands are shown to be present in the gap. In polyparaphenylene, owing to the larger dopant concentration that can be obtained, these bands have widths of 0.55 eV compared to the 0.24- and 0.10-eV widths in polypyrrole and the 0.24- and 0.19-eV widths in polythiophene.

A conduction mechanism based on bipolarons as charge carriers in the highly conducting regime of these compounds[38] is consistent with the vanishingly small Pauli susceptibility reported in the metallic regime of SbF_5-doped polyparaphenylene and the absence of any ESR signal in electrochemically cycled, conducting polypyrrole. The presence of bipolaron bands in the gap is consistent with (i) the electron-energy-loss spectra observed for highly-AsF_5-doped polyparaphenylene, (ii) the evolution of the optical spectra as a function of doping in polypyrrole, and (iii) the electrochromic effect reported in polythiophene.

Although some quantitative aspects might differ, e.g., if explicit introduction of correlation and disorder effects can be made, we are confident that our calculations reliably indicate the major trends occurring upon high doping of conjugated polymers with a nondegenerate ground state.

ACKNOWLEDGMENTS

The authors acknowledge stimulating discussions with Professor R. Silbey, Dr. G. B. Street, Dr. J. C. Scott, Professor A. J. Heeger, and Professor F. Wudl. One of us (J.L.B.) is grateful to the Belgian National Fund for Scientific Research (Fonds National de la Recherche Scientifique) for continuous support. Another one of us (B.T.) thanks Institut pour l'Encouragement de la Recherche Scientifique dans l'Industrie et l'Agriculture (IRSIA, Belgium) for financial support.

[1]For a recent account, see, e.g., Proceedings of the International Conference on the Physics and Chemistry of Conducting Polymers (Les Arcs, France, 1982) [J. Phys. (Paris) Colloq. 44, C3 (1983)].

[2]R. H. Baughman, J. L. Brédas, R. R. Chance, R. L. Elsenbaumer, and L. W. Shacklette, Chem. Rev. 82, 209 (1982).

[3]J. M. André, J. L. Brédas, J. Delhalle, J. Ladik, G. Leroy, and C. Moser eds., *Recent Advances in the Quantum Theory of Polymers,* Vol. 113 of *Lecture Notes in Physics* (Springer, Berlin, 1980).

[4]W. P. Su, J. R. Schrieffer, and A. J. Heeger, Phys. Rev. B 22, 2209 (1980); B 28, 1138(E) (1982).

[5]M. J. Rice, Phys. Lett. 71A, 152 (1979).

[6]D. Moses, A. Denenstein, J. Chen, A. J. Heeger, P. McAndrew, T. Woerner, A. G. McDiarmid, and Y. W. Park, Phys. Rev. B 25, 7652 (1982).

[7]T.-C. Chung, F. Moraes, J. D. Flood, and A. J. Heeger, Phys. Rev. B 29, 2341 (1984).

[8]M. Peo, S. Roth, K. Dransfeld, B. Tieke, J. Hocker, H. Gross, A. Grupp, and H. Sixl, Solid State Commun. 35, 119 (1980).

[9]J. C. Scott, M. Krounbi, P. Pfluger, and G. B. Street, Phys. Rev. B 28, 2140 (1983).

[10]J. L. Brédas, R. R. Chance, and R. Silbey, Mol. Cryst. Liq. Cryst. 77, 319 (1981).

[11]A. R. Bishop, D. K. Campbell, and K. Fesser, Mol. Cryst. Liq. Cryst. 77, 253 (1981).

[12]S. A. Brazovskii and N. Kirova, Zh. Eksp. Teor. Fiz. Pis'ma Red. 33, 6 (1981) [JETP Lett. 33, 4 (1981)].

[13]J. L. Brédas, R. R. Chance, and R. Silbey, Phys. Rev. B 26, 5843 (1982).

[14]J. L. Brédas, J. C. Scott, K. Yakushi, and G. B. Street, Phys. Rev. B (to be published).

[15]J. C. Scott, J. L. Brédas, K. Yakushi, P. Pfluger, and G. B. Street, Synth. Metals 9, 165 (1984).

[16]J. L. Brédas, B. Thémans, and J. M. André, Phys. Rev. B 26, 6000 (1982).

[17]J. L. Brédas, B. Thémans, and J. M. André, Phys. Rev. B 27, 7827 (1983).

[18]C. C. J. Roothaan, Rev. Mod. Phys. 23, 69 (1951).

[19]J. S. Binkley, R. A. Whitehead, P. C. Hariharan, R. Seeger, J. A. Pople, W. J. Hehre, and M. D. Newton, Quantum Chem. Program Exchange 10, 368 (1978).

[20]A. Pullman, H. Berthod, and N. Gresh, Int. J. Quantum Chem. Symp. 10, 59 (1976).

[21]J. L. Brédas, B. Thémans, J. M. André, and G. B. Street (unpublished).

[22]G. B. Street and A. Nazzal (unpublished).

[23]G. J. Visser, G. J. Heeres, J. Wolters, and A. Vos, Acta. Crystallogr. Sect. B 24, 467 (1968).

[24]F. L. Vogel in *Molecular Metals,* Vol. I of *NATO Conference Series VI,* edited by W. E. Hatfield (Plenum, New York, 1979), p. 261.

[25]J. M. André, L. A. Burke, J. Delhalle, G. Nicolas, and P. Durand, Int. J. Quantum Chem. Symp. 13, 283 (1979).

[26]J. L. Brédas, R. R. Chance, R. H. Baughman, and R. Silbey, J. Chem. Phys. 76, 3673 (1982).

[27]J. L. Brédas, R. L. Elsenbaumer, R. R. Chance, and R. Silbey, J. Chem. Phys. 78, 5656 (1983).

[28]J. L. Brédas, B. Thémans, and J. M. André, J. Chem. Phys. 78, 6137 (1983).

[29]L. W. Shacklette, R. R. Chance, D. M. Ivory, G. G. Miller, and R. H. Baughman, Synth. Met. 1, 307 (1979).

[30]L. W. Shacklette, R. L. Elsenbaumer, R. R. Chance, J. M. Sowa, D. M. Ivory, G. G. Miller, and R. H. Baughman, J. Chem. Soc. Chem. Commun. 1982, 361 (1982).

[31]L. W. Shacklette, H. Eckhardt, R. R. Chance, G. G. Miller, D. M. Ivory, and R. H. Baughman, J. Chem. Phys. 73, 4098 (1980).

[32]Y. Delugeard, J. Desuche, and J. L. Baudour, Acta Crystallogr. Sect. B 32, 702 (1976).

[33]J. L. Baudour, H. Cailleau, and W. B. Yelon, Acta Crystallogr. Sect. B 33, 1773 (1977).

[34]J. L. Baudour, Y. Delugeard, and P. Rivet, Acta Crystallogr. Sect. B 34, 625 (1978).

[35]O. Bastiansen, Acta Chem. Scand. 3, 408 (1949).

[36]C. S. Yannoni and T. C. Clarke, Phys. Rev. Lett. 51, 1191

(1983).
[37]J. H. Noordik, J. Schreurs, R. O. Gould, and J. J. Mooij, Pure Appl. Chem. 51, 73 (1979).
[38]R. R. Chance, J. L. Brédas, and R. Silbey, Phys. Rev. B 29, 4491 (1984).
[39]G. Crecelius, M. Stamm, J. Fink, and J. J. Ritsko, Phys. Rev. Lett. 50, 1498 (1983).
[40]K. Fesser, A. R. Bishop, and D. K. Campbell, Phys. Rev. B 27, 4804 (1983).
[41]J. J. Ritsko, Phys. Rev. Lett. 46, 849 (1981).
[42]J. L. Brédas, R. R. Chance, R. Silbey, G. Nicolas, and P. Durand, J. Chem. Phys. 77, 371 (1982).
[43]G. B. Street, T. C. Clarke, M. Krounbi, K. K. Kanazawa, V. Y. Lee, P. Pfluger, J. C. Scott, and G. Weiser, Mol. Cryst. Liq. Cryst. 83, 253 (1982).
[44]G. B. Street, T. C. Clarke, R. H. Geiss, V. Y. Lee, A. Nazzal, P. Pfluger, and J. C. Scott, J. Phys. (Paris) Colloq. 44, C3-599 (1983).
[45]K. J. Wynne and G. B. Street, Ind. Eng. Chem. Proc. Res. Dev. 21, 23 (1982).
[46]A. F. Diaz, K. K. Kanazawa, and G. P. Gardini, J. Chem. Soc. Chem. Commun. 1979, 635.
[47]J. L. Brédas, R. Silbey, D. S. Boudreaux, and R. R. Chance, J. Am. Chem. Soc. 105, 6555 (1983).
[48]T. Yamamoto, K. Sanechika, and A. Yamamoto, J. Polym. Sci. Polym. Lett. Ed. 18, 9 (1980).
[49]J. W. P. Lin, and L. P. Dudek, J. Polym. Sci. Polym. Chem. Ed. 18, 2869 (1980).
[50]M. Kobayashi, J. Chen, T. C. Chung, F. Moraes, A. J. Heeger, and F. Wudl, Synth. Metals (to be published).
[51]G. Tourillon and F. Garnier, J. Electroanal. Chem. 135, 173 (1982).
[52]K. Kaneto, K. Yoshino, and Y. Inuishi, Solid State Commun. 46, 389 (1983).
[53]R. J. Waltman, J. Bargon, and A. F. Diaz, J. Phys. Chem. 87, 1459 (1983).
[54]A. Almenningen, O. Bastiansen, and P. Svendsas, Acta. Chem. Scand. 12, 1671 (1958).
[55]L. Nygaard, J. T. Nielsen, J. Kirchheiner, G. Maltesen, J. Rastrup-Andersen, and G. O. Sorensen, J. Mol. Struct. 3, 491 (1969).
[56]A. F. Diaz, J. Crowley, J. Bargon, G. P. Gardini, and J. B. Torrance, J. Electroanal. Chem. 121, 355 (1981).
[57]M. A. Druy and R. J. Seymour, J. Phys. (Paris) Colloq. 44, C3-595 (1983).
[58]T.-C. Chung, J. H. Kaufman, A. J. Heeger, and F. Wudl (unpublished).